

## Resonant transmission of microwaves through a hexagonal array of holes in a thin metal layer

J R Suckling<sup>1,3</sup>, J R Sambles<sup>1</sup> and C R Lawrence<sup>2</sup>

<sup>1</sup> School of Physics, Exeter University, Devon, EX4 4QL, UK

<sup>2</sup> QinetiQ, Cody Technology Park, Farnborough, GU14 0LX, UK

E-mail: [J.R.Suckling@ex.ac.uk](mailto:J.R.Suckling@ex.ac.uk)

*New Journal of Physics* **9** (2007) 101

Received 26 June 2006

Published 25 April 2007

Online at <http://www.njp.org/>

doi:10.1088/1367-2630/9/4/101

**Abstract.** Resonant transmission of microwaves through a hexagonal array of holes in a very thin aluminium layer is studied. The array of holes, with diameter much less than the incident wavelength, leads to a strong transmission peak at a frequency just lower than the diffraction limit of the array. The results are well-modelled using a finite element package. The effect of metal depth on transmission intensity and the maximum efficiency of the hole array is also explored. Further experimental data are presented for the transmission of microwaves as a function of angle of incidence. It is shown that strong transmission occurs at frequencies just lower than the diffraction edges of the array. Incidentally, it is also shown that less than 0.01% of normally incident microwave radiation is transmitted through a continuous metal layer of thickness only 40% of the skin depth.

### Contents

<b>1. Introduction</b>	<b>2</b>
<b>2. Results and discussion</b>	<b>3</b>
2.1. Normal incidence resonant transmission of the hole array . . . . .	3
2.2. Angle-dependent resonant transmission of the hole array. . . . .	8
<b>3. Conclusions</b>	<b>10</b>
<b>Acknowledgments</b>	<b>10</b>
<b>References</b>	<b>10</b>

<sup>3</sup> Author to whom any correspondence should be addressed.

## 1. Introduction

Enhanced transmission of photons through a regular array of subwavelength holes in an otherwise opaque screen has been an area of significant interest since it was first demonstrated by Ebbesen *et al* [1]. The transmission through each hole was significantly higher than that expected from simple analytical theory [2]. Indeed, the amount of light transmitted by the structure is significantly more than that arriving over the integrated area of the holes. Enhanced transmission peaks were located at a frequency below the diffraction limit of the array, which is dictated by the array pitch. Hence, the enhanced transmission was deemed to be the result of the large electric fields of surface plasmon polaritons (SPPs), at both the incident and transmitted half space interfaces, enhancing the evanescent fields within each hole. This allows a greater energy to couple into the transmitted beam than might be expected if direct transmission of the holes were considered alone. Subsequent work mapped the frequency dispersion of the hole array, confirming that SPPs aided the transmission [3]. Theoretical work [4] strengthened the SPP link by showing that no guided modes could be supported within a subwavelength hole. Further verification has been provided both theoretically and experimentally [5]–[7]. Theoretical work on random arrays of holes demonstrated that the regular array of holes was essential in the enhanced transmission, and without the array only weaker localized surface plasmons could exist round the rim of each hole [8]. The transmission spectrum of an array of holes has also been explored with the added assumption that the SPP is supported only on one surface of the array [9]. This demonstrated a simplified transmission spectrum, different to that shown in [1], lacking features due to coupling of SPPs between both surfaces of the array.

Work on varying dimensional aspects of the array has been explored in detail. The dependence of the transmission on array depth has been studied both experimentally and theoretically [10], [11]. Further dependence on the material properties of the array has been explored [12]. The dependence of the transmission on hole shape has also been studied [13]. Furthermore, the enhanced transmission of photons through subwavelength holes has been extended to longer wavelength, notably into the infrared [14], [15], the terahertz regime [16]–[18] and the microwave regime [19]. It is worth noting that while all of the arrays in the lower frequency regimes used metal, or semiconductor, layers which were thinner than the wavelength of the incident light, none to date have explored the transmission of an array in a sub skin depth thickness material, where, in this case, the skin depth is less than 0.01 of the wavelength.

The work presented here is an experimental investigation into the enhanced transmission of microwaves through a hexagonal array of holes in a metal layer which is much thinner than the skin depth of the microwaves. Transmission spectra of two orientations of microwave polarization relative to the hole array are measured. The experimental data are complemented by numerical computer modelling, allowing the detailed exploration of the resonant fields supported by the structure. Further angle-dependent data are explored to show that it is the formation of SPPs on the array surface that facilitates the enhanced transmission. The work also demonstrates a strong screening of the incident microwaves by a metal layer of a thickness that might be expected to transmit a significant proportion of the incident power.

Transmission of electromagnetic radiation through a single subwavelength circular hole in an opaque screen becomes increasingly prohibitive when the wavelength of the incident radiation becomes larger than the radius of the hole. As only evanescent modes are supported inside the holes in this regime the transmission intensity is expected to fall as  $(r/\lambda)^4$  [2], where  $r$  is the hole radius. However, creating a periodic array of holes allows coupling to a bound surface mode, the

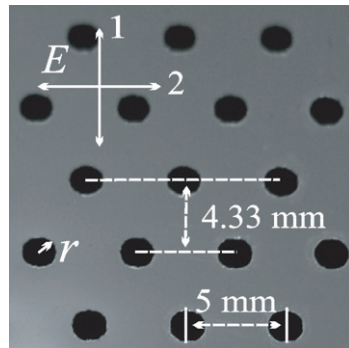


**Figure 1.** Photograph of a section of the sample, with dimensions marked. Both incident electric polarizations are marked.

surface plasmon, by scattering off the array. This increases the intensity of the transmission by greatly enhancing the fields at the surface of the array [3]–[5], [10], [11]. As a further result of coupling to the surface plasmon the transmission peak is produced at wavelengths slightly longer than the pitch of the array [1]. For a hexagonal array of holes the pitch is equal to the separation of the rows of holes, or  $d \cos 30^\circ$ , where  $d$  is the nearest neighbour distance and  $30^\circ$  is the angle between the normal of one row and the line connecting to the nearest hole in an adjacent row.

## 2. Results and discussion

### 2.1. Normal incidence resonant transmission of the hole array

Figure 1 is a photograph of a portion of the sample with dimensions and the two orthogonal polarizations of incident microwaves marked. Two samples are investigated separately, for one the normal incidence transmission is explored and for the other the angle dependence. Both hexagonal arrays of circular holes are cut using a laser etching system with a substrate comprising a  $50 \mu\text{m}$  thick flexible dielectric film on to which  $\sim 150 \text{ nm}$  of aluminium has been deposited by evaporation. The laser etcher uses a template in which each hole has a radius,  $r = 0.796 \text{ mm}$ . The sample used for normal incidence experimentation has a nearest neighbour separation of  $5 \text{ mm}$  (a pitch of  $4.33 \text{ mm}$ ), whereas that used to explore angle-dependent transmission has a hole separation of  $7.5 \text{ mm}$  (a pitch of  $6.495 \text{ mm}$ ). Both sheets are cut to form an array  $\sim 27 \times 21.5 \text{ cm}$  in size. The samples are then illuminated with a collimated microwave beam, which has a beam spot of about  $15 \text{ cm}$  diameter, smaller than the full array size to minimize undesirable edge effects. The collimating mirrors are positioned in the far field so that only transmission parallel to the incident beam is measured. A well collimated beam is essential to avoid the beam divergence shifting the transmission peak to a lower frequency; caused by an enhancement of the in-plane photon momentum parallel to the array surface due to wave-front curvature. The data range studied was  $50 < f < 75 \text{ GHz}$  ( $4.00 < \lambda < 6.00 \text{ mm}$ ). Theoretical modelling has been undertaken with a finite element method (FEM) program, Ansoft's high frequency structure simulator (HFSS) (HFSS, Ansoft Corporation, Pittsburg, PA, USA). The FEM model mimics the physical structure of the sample as closely as possible. (Note, for frequencies above the diffraction limit the transmitted power modelled exceeds that detected in the experiment, since in the experiment only the zero order beam is detected.)

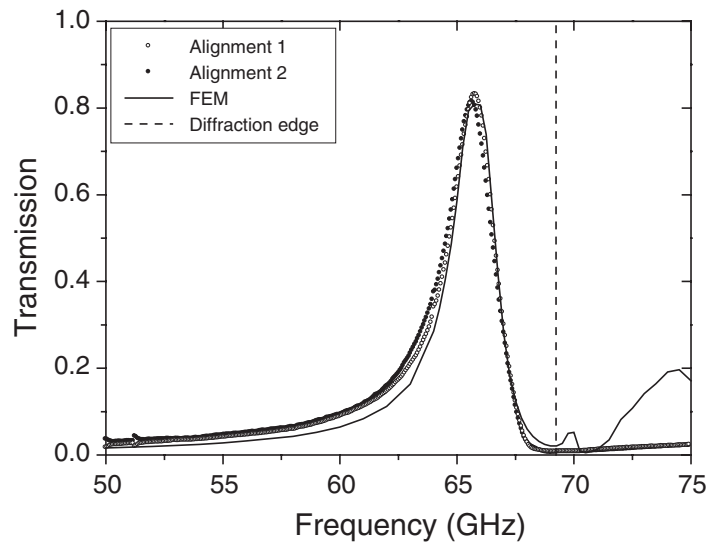


**Figure 2.** Experimental data for normally incident microwaves in two orthogonal polarizations, marked 1 and 2 in figure 1, shown as open and filled circles respectively. FEM model results for hole radii  $\bar{r} = 0.891$  mm,  $\delta r \pm 0.028$  mm is the solid line. The diffraction limit of the array at 69.2 GHz is the vertical dashed line.

Figure 2 shows the experimental transmittance of normally incident microwaves as a function of frequency for the first sample. Data for two orthogonal polarizations of microwaves are presented (filled and hollow dots), as marked in figure 1. It is clear that the very strong transmission ( $\sim 80\%$  at the peak) and the overall form of the transmission spectrum is independent of polarization orientation at normal incidence. The diffraction limit of the array is marked as the vertical dotted line at 69.2 GHz. Finally, the FEM modelled data is shown as the solid line. As the array was manufactured by laser etching holes into the metal and dielectric it is inevitable that there will be some spread of the hole radii across the sample. This is dependent on slight variations in the metal or dielectric thickness, altering the etch rate, and variations in the focus of the laser at different points on the sample. To model this spread of hole size, many separate FEM models were created each with a different hole size. The outputs for each hole size were combined by a weighted Gaussian average. As the laser was focused on the outer limit of the 0.796 mm radius it was assumed that the hole radii could only be larger. The final result uses a Gaussian spread of hole sizes centred around a hole radius,  $r = 0.891$  mm with a full width half maximum encompassing the range  $0.863 < r < 0.919$  mm. Using this weighted averaging gave a model response, the continuous line in figure 2, that agrees very well with the data.

In the transmission spectrum shown in figure 2, the strong transmission peak is located below the diffraction limit of the array. This is consistent with the SPP-mediated transmission reported by Ebbesen *et al* [1]. No other transmission peaks are recorded at lower frequencies; which might have been attributed to the surface plasmon existing at the metal/dielectric substrate interface, discussed in [1]. This shows that the thin dielectric layer supporting the aluminium has negligible effect on the microwave transmission; effectively the lower interface is a slightly perturbed metal/air interface.

Note in passing, the very low transmission of the continuous metal layer, which was never measured to rise above 0.01% of the incident beam power across the entire

frequency range. In the microwave regime the skin depth,  $\delta$ , can be approximated by  $\delta = \sqrt{2/\mu_0\omega g}$  [20], where  $g$  is the metal conductivity and  $\omega$  is the frequency at which the skin depth is measured. For aluminium with  $g = 3.8 \times 10^7 \text{ S m}^{-1}$ , this gives a skin depth of  $\sim 400 \text{ nm}$  at a frequency of 50 GHz [20]. Naïvely we might expect a layer with a thickness equal to the skin depth to transmit  $\sim 36\%$  of incident radiation and thus anticipate that 150 nm of aluminium would be quite transmissive. It is of course the massive impedance mismatch between the aluminium layer and the surrounding air that prevents transmission and not the metal thickness; indeed even 20 nm of aluminium will reflect over 99% at these frequencies.

To effectively model such thin layers of metal with the FEM program it was necessary to use a surface impedance approximation (SIA) to describe the response of the metal layer instead of incorporating finite elements into the metal. When the metal is described by finite elements within the 150 nm depth, compared to the 6 mm wavelength scales of the rest of the model, the computation time becomes prohibitive. The SIA simplifies the problem by using the conductivity of the metal to approximate the absorption of electromagnetic radiation within the skin depth. Crucially, not only does the SIA reduce the problem size, but it also forbids penetration of the electromagnetic fields into the metal layer. The fact that the model shows such good agreement with experimental data for the transmission through such thin metallic layers further implies that there is negligible penetration of the electromagnetic fields into the metal layer, either from the incident wave or from any surface modes. As already indicated, even though the skin depth of the metal in the microwave regime is significantly greater than the metal thickness of the sample, the impedance mismatch at the metal/air interface screens out the microwaves very effectively. Therefore, all the transmission of microwaves can be considered as occurring solely through the holes of the array. This is perhaps a surprising result, given the extremely thin nature of the metal layer. Figure 3 shows the Poynting vector plot on a vertical plane parallel to the incident polarization of an array of holes with  $r = 0.875 \text{ mm}$  at a resonant frequency of 66 GHz. The metal layer is represented by the broken black line. Figure 3 clearly shows the coupling of the microwaves to surface modes (represented by the enhanced power flow along the surface of the array) and the channelling of the microwaves through the holes of the array. The cross-section of the diagram with respect to the array is also shown in figure 3.

From the above discussion it may appear that the aluminium is behaving as a perfect metal and thus that the surface plasmon in this experiment is reminiscent of the spoof plasmons predicted by Pendry [21] and observed by Hibbins *et al* [22]. However, unlike [21, 22], in which both the periodicity and the dimensionality of the holes cut into the perfect metal are required to be subwavelength in size, the periodicity of the array within this hexagonal array is crucial to the coupling of the microwaves into the surface plasmons mode and, thus, is of the order of the experimental wavelength. In that respect the plasmons within this work are treated as being genuine, not spoof.

Figure 4 is an extension to the FEM model showing the effect of metal thickness on transmission intensity. This particular model contains holes with radius,  $r = 0.915 \text{ mm}$ . The thickness of the aluminium layer is varied from 225 nm to 2 mm. It is immediately clear that there is a limit to the increase in the intensity of transmission of the microwaves. Below  $\sim 2 \mu\text{m}$  the thickness of the metal layer no longer significantly attenuates the signal transmitted through the holes. The evanescent decay of the electromagnetic fields within the holes becomes negligible below this metal thickness. A hexagonal array of hole radius 0.915 mm and hole spacing of 5 mm has a maximum efficiency of  $\sim 93\%$  at 65.4 GHz for a thin metal layer on a  $50 \mu\text{m}$  dielectric substrate. This efficiency represents a transmission of 75 times more than the radiation directly

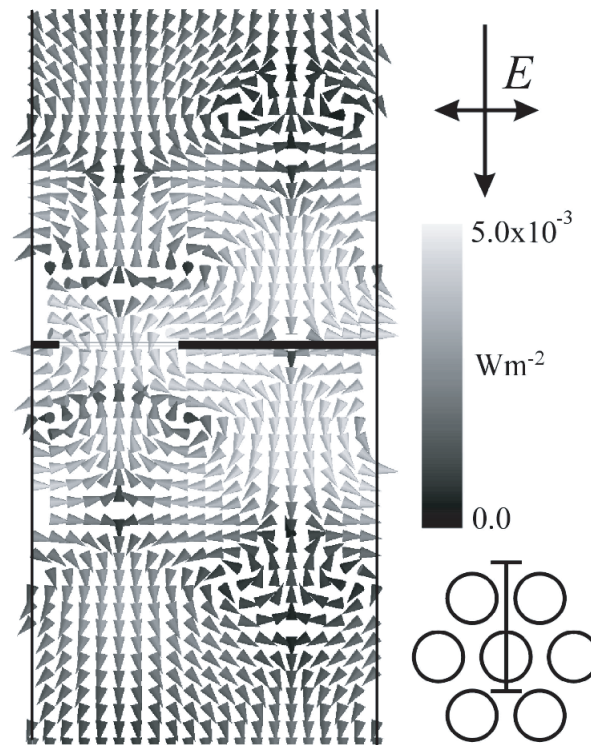


**Figure 3.** FEM field profile showing power flow through a hole of radius 0.915 mm. Field profile cross-section and incident beam direction and polarization marked. Array sample not to scale.

incident on the area of the holes. This FEM modelled peak efficiency is higher than recorded experimentally simply because the spread of hole size within the experimental array broadens the resonance, therefore reducing the peak transmission intensity of the array.

A further feature of note is the transmission peak present, at  $\sim 70$  GHz, in the FEM modelled data, but not in the experimental data, figures 4 and 2 respectively. Initially assumed to be an artefact of the treatment of diffracted orders within HFSS, in figure 4 this feature actually reduces in frequency to *below* the diffraction limit as the film thickness is increased. Clearly another explanation is needed. Genet *et al* [9] discuss the transmission spectrum of an array of holes when only considering a surface plasmon resonant state on the incident surface of the array. This gave a similar response to the experimental data presented within this paper, inasmuch as the spectrum consisted of a main resonance below the diffraction limit, and also no resonance above it. As HFSS uses a complete model of the system to predict the resonant response then some difference between the HFSS modelling, Genet *et al* modelling and experimental data has to be found to account for the lack of the higher frequency mode. Figures 5(a) and (b) show the instantaneous electric field direction, on an array with an aluminium depth of 1 mm, for the two resonances; one below the diffraction limit, at 68.25 GHz (a), and the other above the diffraction limit at 69.25 GHz (b). It is clear that the modes constitute a symmetric, anti-symmetric pair. However, as stated, HFSS reduces solution time by describing the metal using an SIA; it does not allow any penetration of the electric fields into the metal. By contrast, the experimental sample, having been heat etched by a laser, is likely to have a thinner metal region round the hole due to

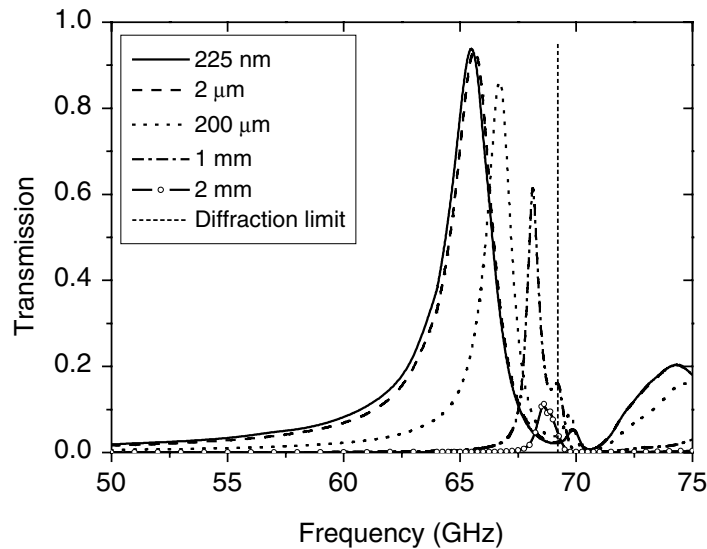


**Figure 4.** FEM data of resonant transmission against metal layer depth, varied from 225 nm to 2 mm, for a hexagonal array with hole radius 0.915 mm.

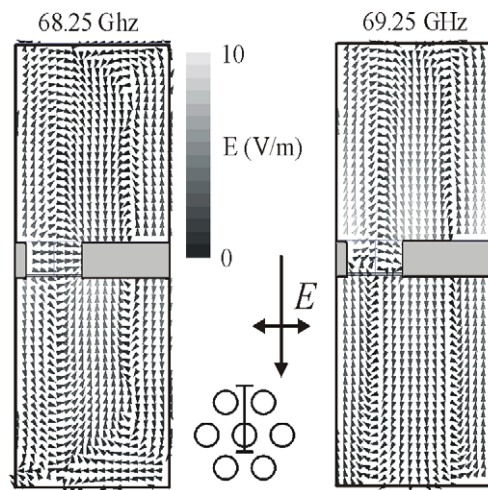


**Figure 5.** Instantaneous electric vector of transmission maxima located at 68.25 GHz and 69.25 GHz (figure 4). Sample has hole radius  $r = 0.915$  mm and metal depth = 1 mm. Sample cross-section and incident beam shown. Cross-section not to scale.

the damage by the laser beam. This would allow the opposing electric fields of the anti-symmetric mode to penetrate into the thinner metal layer and cancel out. Thus, the extra mode, found in the theory, is weakened and not found in practice. Figure 6 shows the frequency of the pair of modes as a function of metal depth, for the range  $150 \text{ nm} < d_{\text{aluminium}} < 2000 \text{ }\mu\text{m}$ . It can be seen that as the metal depth increases the modes approach each other. This would be expected as, in the limit of an infinitely thick metal layer, the surface plasmon resonance could be considered as only existing on one surface; this also explains why Genet *et al* do not predict this mode.

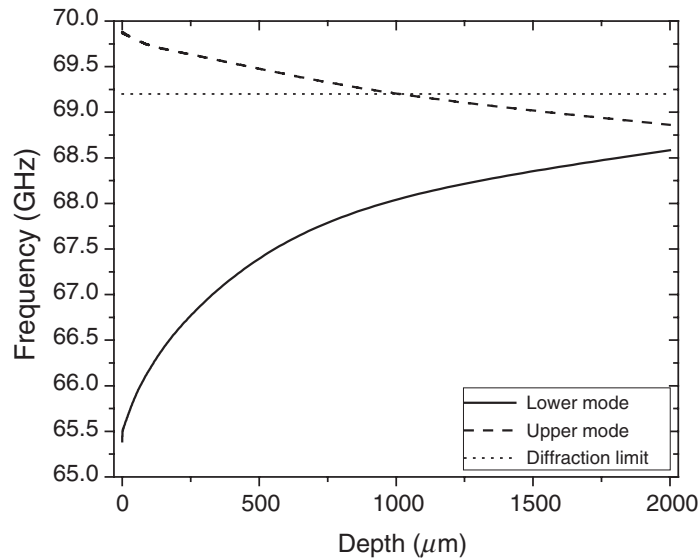


**Figure 6.** Modelled data showing frequencies of upper and lower coupled modes as a function of metal depth (dashed and solid lines respectively). Depth over range  $225 \text{ nm} < d_{\text{aluminium}} < 2 \text{ mm}$ , hole radius  $0.915 \text{ mm}$ . Diffraction limit shown at  $69.2 \text{ GHz}$  (dotted line).

## 2.2. Angle-dependent resonant transmission of the hole array

Angle-dependent transmission was explored with the second sample. Both  $p$ - and  $s$ -polarized incident photons were studied for two different initial alignments of the incident photon electric component on the sample (labelled in figure 1 as 1 and 2). The work presented in the previous section showed the resonant transmission of an array with a  $5 \text{ mm}$  hole separation. This section will show the angle-dependent data for an array with a  $7.5 \text{ mm}$  hole separation. The increased pitch of the array ( $p = 6.495 \text{ mm}$ ) not only reduces the main resonant mode frequency to  $f = 46.16 \text{ GHz}$ , but also brings an increased number of diffracted orders into the frequency and angle range studied,  $50 < f < 75 \text{ GHz}$  and  $-60 < \theta < +60^\circ$  respectively. This will allow for a clearer comparison between the diffraction edges and the transmission maxima of the hole array.

Figures 7(a)–(d) show the angle-dependent transmission data for the hole array, with the  $7.5 \text{ mm}$  hole separation. Figure 7(a) shows the transmission of microwaves whose electric component is aligned along direction 1, as shown in figure 1, and whose angle of incidence is varied such that the microwaves are  $p$ -polarized with respect to the sample surface. Figure 7(b) shows the same plane of incidence, but this time the polarization of the microwaves is rotated by  $90^\circ$  round the incident beam direction to be  $s$ -polarized. Diffraction edges are marked by the different styled lines and labelled with the appropriate scattering orders. The reciprocal lattice corresponding to this plane of incidence is shown in figure 8(a), with the corresponding scattering orders marked. Firstly, it is clear that the transmission peaks occur only at lower frequencies than those of the diffraction edges, consistent with the spectra shown in figure 2 and the assertion that SPPs mediate the transmission. It is also clear that the  $p$ -polarized microwaves couple into a greater number of scattered orders than those which are  $s$ -polarized. This difference is due to the coupling conditions of the array. Microwaves can couple into a transmitted diffracted order

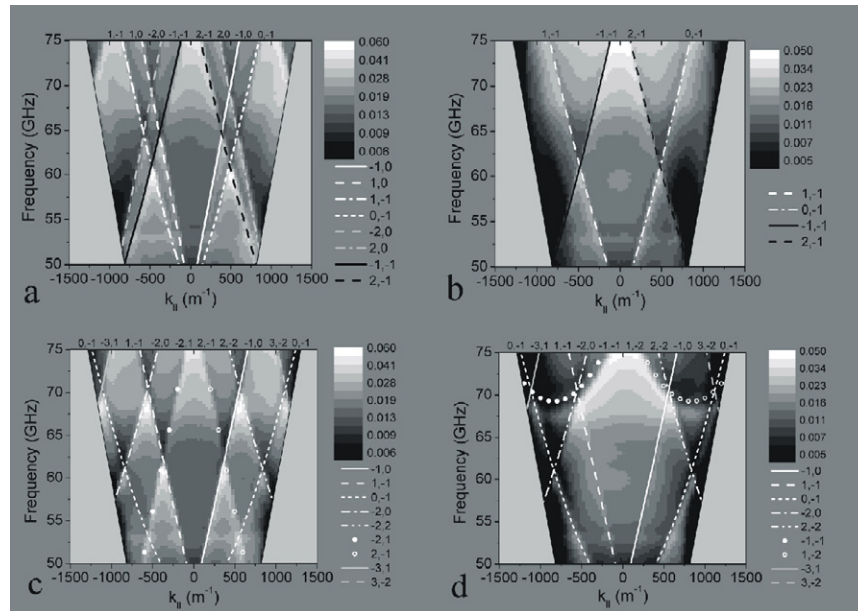


**Figure 7.** Experimental data showing the angle-dependent transmission of microwaves through an array with 7.5 mm hole spacing. Polarization orientations are as in figure 1: (a) alignment 1,  $p$ -polarized transmission data; (b) alignment 2,  $s$ -polarized; (c) alignment 2,  $p$ -polarized; and (d) alignment 1,  $s$ -polarized. Data shown as a function of in-plane wavevector over the range  $-1500 < k_{\parallel} < 1500 \text{ m}^{-1}$  and frequency  $50 < f < 75 \text{ GHz}$ .

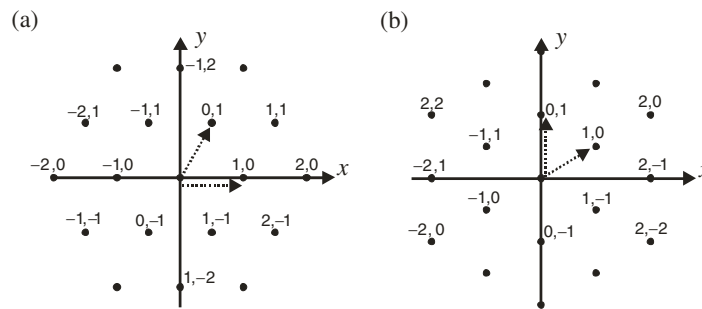


**Figure 8.** Reciprocal lattices from which the diffraction edges, shown in figure 7, are derived. Lattice (a) corresponds to figures 7(a) and (b). Lattice (b) corresponds to figures 7(c) and (d).

provided that a component of the incident photon's electric field is parallel to the grating vector from which it might scatter, in real space, or perpendicular to the array surface. The second condition is satisfied by  $p$ -polarized photons for all scattering orders, while the first is satisfied by  $s$ -polarized photons except for scattering orders located along the  $x$ -axis in reciprocal space. Figures 7(c) and (d) show the  $p$ - and  $s$ -polarized transmission, respectively, of the hexagonal array of holes when the plane of incidence is rotated by  $\phi = 90^\circ$  around the normal axis with respect to the sample surface. Now the  $p$ -polarized microwaves are aligned along direction 2 (figure 1) and the  $s$ -polarized photons along direction 1 (figure 1). The reciprocal lattice shown

in figure 8(b) corresponds to the scattering orders marked in figures 7(c) and (d). Once again the *s*-polarized photons may only couple into diffracted orders when a component of the photon's electric field is parallel to the grating vector, therefore photons do not excite orders with centres located on the *x*-axis in the reciprocal lattice. However, there is a further curiosity in the lack of either the  $(-1, -1)$  or  $(1, -2)$  in the *p*-polarized diffraction data, figure 7(c). Considering that these modes are the result of second order scattering it must be assumed their absence is due to low coupling efficiency.

### 3. Conclusions

In summary, the resonant transmission of microwaves through a hexagonal array of holes cut into a very thin metal layer on a thin dielectric backing has been presented. It has been shown that the array supports very strong resonant transmission peaks at frequencies just below that of the diffraction limit of the array. These transmission peaks are independent of polarization orientation on the sample for a normally incident microwave beam. It has also been shown that a continuous thin metal layer, which is much less than the skin depth of the microwaves, blocks the incident microwaves so effectively that no transmitted signal can be measured. It appears that all transmission of the array occurs through the holes only, with no measurable field leakage through the metal itself, despite the enhanced surface fields. The impedance mismatch between the air and the metal prevents significant penetration of the fields into the metal. The transmittance of the array is shown to increase as the hole depth is reduced for a given hole size, but that a maximum transmittance of 93% is reached for a metal thickness of  $2\ \mu\text{m}$  or less ( $>750\%$  of the incident radiation falling on the holes). The effect of metal thickness has also been discussed in relation to the resonant frequency and it has been shown that, in theory, there are two resonant features which are a pair of symmetric and anti-symmetric modes. The absence of the weaker, higher frequency mode from the experimental data may be due to some weak penetration of the electric fields within the extremely thin metal at the edges of the holes, disrupting the resonant fields. Finally, the angle-dependent transmission of microwaves through the holes has been presented for an array with a larger hole separation (7.5 mm). It has been shown that strong transmission occurs close to the diffraction edges. Furthermore, it is shown that while *p*-polarized photons may couple into any available diffracted order, *s*-polarized photons are limited to the orders whereby a component of the incident *E*-field is parallel to the grating vector.

### Acknowledgments

We thank both the Engineering and Physical Sciences Research Council (EPSRC) and the QinetiQ Fellow's Stipend Fund for their financial support.

### References

- [1] Ebbesen T W, Lezec H, Ghaemi H F, Thio T and Wolff P A 1998 *Nature* **391** 667
- [2] Bethe H A 1944 *Phys. Rev.* **66** 163
- [3] Ghaemi H F, Thio T, Grupp D E, Ebbesen T W and Lezec H J 1998 *Phys. Rev. B* **58** 6779
- [4] Popov E, Neviere M, Enoch S and Reinisch R 2000 *Phys. Rev. B* **62** 16100
- [5] Darmanyany S A and Zayats A V 2003 *Phys. Rev. B* **67** 035424

- [6] Sarrazin M, Vigneron J-P and Vigoureux J-M 2003 *Phys. Rev. B* **67** 085415
- [7] Barnes W L, Murray W A, Dintinger J, Devaux E and Ebbesen T W 2004 *Phys. Rev. Lett.* **92** 107401
- [8] Sarychev A K, Podolskiy V A, Dykhne A M and Shalaev V M 2002 *IEEE J. Quantum Electron.* **38** 956
- [9] Genet C, van Exter M P and Woerdman J P 2003 *Opt. Commun.* **225** 331
- [10] Degiron A, Lezec H J, Barnes W L and Ebbesen T W 2002 *Appl. Phys. Lett.* **81** 4327
- [11] Martin-Moreno L, Garcia-Vidal F J, Lezec H J, Pellerin K M, Thio T, Pendry J B and Ebbesen T W 2001 *Phys. Rev. Lett.* **86** 1114
- [12] Grupp D E, Lezec H J, Ebbesen T W, Pellerin K M and Thio T 2000 *Appl. Phys. Lett.* **77** 1569
- [13] Schuchinsky A G, Zelenchuk D E and Lerer A M 2005 *J. Opt. A: Pure Appl. Opt.* **7** 102
- [14] Ye Y-H and Zhang J-Y 2004 *Appl. Phys. Lett.* **84** 2977
- [15] Williams S M, Stafford A D, Rogers T M, Bishop S R and Coe J V 2004 *Appl. Phys. Lett.* **85** 1472
- [16] Rivas J G, Schotsch C, Bolivar P H and Kurz H 2003 *Phys. Rev. B* **68** 201306
- [17] Cao H and Nahata A 2004 *Opt. Express* **12** 1004
- [18] Janke C, Rivas J G, Schotsch C, Beckmann L, Bolivar P H and Kurz H 2004 *Phys. Rev. B* **69** 205314
- [19] Beruete M, Sorolla M, Campillo I, Dolado J S, Martin-Moreno L, Bravo-Abad J and Garcia-Vidal F J 2004 *Opt. Lett.* **29** 2500
- [20] Reitz J R, Milford F J and Christy R W 1993 *Foundations of Electromagnetic Theory* 4th edn (Reading, MA: Addison-Wesley)
- [21] Pendry J B 2004 *Science* **305** 847
- [22] Hibbins A P, Evans B R and Sambles J R 2005 *Science* **308** 670